Hindawi Publishing Corporation
Discrete Dynamics in Nature and Society
Volume 2015, Article ID 836402, 12 pages
http://dx.doi.org/10.1155/2015/836402

Research Article

Qualitative Analysis of a Quadratic Integrate-and-Fire Neuron Model with State-Dependent Feedback Control

Guangyao Tang,[1] Jin Yang,[2] and Sanyi Tang[3]

[1]*Key Laboratory of Biologic Resources Protection and Utilization, Hubei Minzu University, Enshi, Hubei 445000, China*
[2]*Department of Mathematics, Chongqing Jiaotong University, Chongqing 400074, China*
[3]*College of Mathematics and Information Science, Shaanxi Normal University, Xi'an 710062, China*

Correspondence should be addressed to Guangyao Tang; tgy0201227@163.com

Received 7 May 2015; Revised 14 August 2015; Accepted 30 August 2015

Academic Editor: Michael Radin

Copyright © 2015 Guangyao Tang et al. This is an open access article distributed under the Creative Commons Attribution License, which permits unrestricted use, distribution, and reproduction in any medium, provided the original work is properly cited.

Spiking neuron models which exhibit rich dynamics are usually defined by hybrid dynamical systems. It is revealed that mathematical analysis of these models has important significance. Therefore, in this work, we provide a comprehensively qualitative analysis for a quadratic integrate-and-fire model by using the theories of hybrid dynamical system. Firstly, the exact impulsive and phase sets are defined according to the phase portraits of the proposed model, and then the Poincaré map is constructed. Furthermore, the conditions for the existence and stability of an order 1 periodic solution are provided. Moreover, the existence and nonexistence of an order k ($k \geq 2$) periodic solution have been studied theoretically and numerically, and the results show that the system has periodic solutions with any period. Finally, some biological implications of the mathematical results are discussed.

1. Introduction

To understand the working mechanism of the brain, it is necessary to combine experimental studies of nervous systems with numerical simulations of neuron models [1]. Therefore, a large number of differential equations have been proposed to model neurons in the neurocomputing community. However, there are two major impediments in computational neuroscience including the need for a computationally simple and biologically realistic model of the neuron [2]. To conquer these issues, FitzHugh and Nagumo introduced a new neuron model with cubic nonlinearity and two variables [3, 4]. Then this novel model was reduced to a class of nonlinear bidimensional spiking models with adaptation by many authors which are mathematically tractable, are efficiently implemented, and are able to reproduce many electrophysiological signatures [5–7]. These models often consist of two variables: the membrane potential of the neuron $v(t)$ and the adaptation variable $u(t)$. In this paper, the leak and spike initiation currents function $F(v)$ is assumed to be v^2; then the quadratic adaptive model can be described by the following ordinary differential equations:

$$\begin{aligned} \frac{dv(t)}{dt} &= I + v^2(t) - u(t), \\ \frac{du(t)}{dt} &= a(bv(t) - u(t)), \end{aligned} \tag{1}$$

where I represents the input intensity of the neuron, $1/a$ ($a > 0$) is the characteristic time of the adaptation variable, and b accounts for the interaction between the membrane potential and the adaptation variable. System (1) has been recently used by Izhikevich and Edelman in very large-scale simulations of neural networks [7]. In addition, the rich dynamics that system (1) presented have been investigated in detail by many authors [2, 8, 9].

In view of the spike and reset condition, a spike is emitted at time t when the membrane potential $v(t)$ reaches a threshold (or a cutoff value) v_p. Then the membrane potential is reset to a constant value c and the adaptation variable is

updated to $u(t)+d$. Therefore, system (1) combining with the reset process can be written as

$$\begin{aligned} \frac{dv(t)}{dt} &= I + v^2(t) - u(t), \\ \frac{du(t)}{dt} &= a(bv(t) - u(t)), \\ & \qquad v(t) < v_p, \\ v(t^+) &= c, \\ u(t^+) &= u(t) + d, \\ & \qquad v(t) = v_p, \end{aligned} \tag{2}$$

where d ($d > 0$) describes the total amount of outward minus inward currents activated during the spike and c is the reset membrane potential. System (2) is a hybrid dynamical system which is also known as a planar impulsive semidynamical system (ISDS) [10, 11]. Recently, Shlizerman and Holmes have studied system (2) and obtained explicit approximations of instantaneous firing rates for fixed values of the recovery variable, and then they used the averaging theorem to obtain asymptotic firing rates as a function of current and reset parameters, which provided explicit tools for the interpretation of different spiking patterns [8], whereas Touboul and Brette constructed an adaptation map to study the patterns of spikes numerically when the adaptation variable blows up [2].

In this paper, the global dynamical behaviors of system (2) will be studied theoretically. To this end, some useful definitions and lemmas of the planar ISDS will be presented in Section 2; then we will briefly review the rich dynamics of system (1). In Section 3, we present our main results. In particular, the impulsive and phase sets will be defined exactly in consideration of the phase portraits of model (1) in Section 3.1. In Section 3.2, the Poincaré map for impulsive point series defined in the exact phase set is obtained. In Section 3.3, the existence and stability of order 1 periodic solution will be addressed in detail. In Section 3.4, the existence of order k ($k \geq 2$) periodic solutions will be studied theoretically and numerically. In the last section, Section 4, the related biological implications are discussed from a neurocomputational point of view.

2. Preliminaries and Main Properties of System (1)

The generalized planar ISDS with state-dependent feedback control can be described as follows:

$$\begin{aligned} \frac{dx(t)}{dt} &= P(x, y), \\ \frac{dy(t)}{dt} &= Q(x, y), \\ & \qquad (x, y) \notin \mathcal{J}, \\ x^+ &= I_1(x, y), \\ y^+ &= I_2(x, y), \\ & \qquad (x, y) \in \mathcal{J}, \end{aligned} \tag{3}$$

where $(x, y) \in R^2$. We denote $x^+ = x(t^+)$ and $y^+ = y(t^+)$ for simplicity, and P, Q, I_1, and I_2 are continuous functions from R^2 into R, and $\mathcal{J} \subset R^2$ denotes the impulsive set. For each point $z(x, y) \in \mathcal{J}$, the map $I : R^2 \to R^2$ is defined:

$$I(z) = z^+ = (x^+, y^+) \in R^2, \tag{4}$$

and z^+ is called an impulsive point of z.

Let $\mathcal{P} = I(\mathcal{J})$ be the phase set (i.e., for any $z \in \mathcal{J}$, $I(z) = z^+ \in \mathcal{P}$), and $\mathcal{P} \cap \mathcal{J} = \emptyset$. System (3) is generally known as a planar ISDS. We note that system (2) is an ISDS, where impulsive set $\mathcal{J} = \{(v, u) \in R^2 \mid v = v_p,\ -\infty \leq u \leq I + c^2\}$ is a closed subset of R^2 and continuous function $I : (v_p, u) \in \mathcal{J} \to (v^+, u^+) = (c, u + d) \in R^2$. It follows that the phase set

$$\begin{aligned} \mathcal{P} &= I(\mathcal{J}) \\ &= \left\{(v^+, u^+) \in R^2 \mid v^+ = c,\ -\infty \leq u^+ \leq I + c^2 + d\right\}. \end{aligned} \tag{5}$$

Without loss of generality, unless otherwise specified we assume the initial point $(v_0^+, u_0^+) \in \mathcal{P}$.

In the following we briefly list some definitions related to ISDS, which are useful in this work.

Let (X, Π, R) or (X, Π) be a semidynamical system [10, 11], where X is a metric space and R is the set of all nonnegative reals. For any $z \in X$, the function $\Pi : R \to X$ is a continuous function such that $\Pi(z, 0) = z$ for all $z \in X$, and $\Pi(\Pi(z, t), s) = \Pi(z, t + s)$ for all $z \in X$ and $t, s \in R$ (denoted by $\Pi_z(t) = \Pi(z, t)$). The set $C^+(z) = \{\Pi(z, t) \mid t \in R\}$ is called the positive orbit of z. For any set $\mathcal{J} \subset X$, let $\mathcal{J}^+(z) = C^+(z) \cap \mathcal{J} - \{z\}$ and $\mathcal{J}^-(z) = G(z) \cap \mathcal{J} - \{z\}$, where $G(z) = \cup\{G(z, t) \mid t \in R\}$ and $G(z, t) = \{w \in X \mid \Pi(w, t) = z\}$ is the attainable set of z at $t \in R$. Finally, we set $\mathcal{J}(z) = \mathcal{J}^+(z) \cup \mathcal{J}^-(z)$. Before discussing the dynamical behavior of system (2), we need the following definitions and lemmas [12–16].

Definition 1. An ISDS $(X, \Pi; \mathcal{J}, I)$ consists of a continuous semidynamical system (X, Π) together with a nonempty closed subset $\mathcal{J}$ (or impulsive set) of X and a continuous function $I : \mathcal{J} \to X$ such that the following property holds:

(i) No point $z \in X$ is a limit point of $\mathcal{J}(z)$,

(ii) $\{t \mid G(z, t) \cap \mathcal{J} \neq \emptyset\}$ is a closed subset of R.

Throughout the paper, we denote the points of discontinuity of Π_z by $\{z_n^+\}$ and call z_n^+ an impulsive point of z_n.

We define a function Φ from X into the extended positive reals $R \cup \{\infty\}$ as follows: let $z \in X$; if $\mathcal{J}^+(z) = \emptyset$ we set $\Phi(z) = \infty$; otherwise $\mathcal{J}^+(z) \neq \emptyset$ and we set $\Phi(z) = s$, where $\Pi(x, t) \notin \mathcal{J}$ for $0 < t < s$ but $\Pi(z, s) \in \mathcal{J}$.

Definition 2. A trajectory Π_z in $(X, \Pi, \mathcal{J}, I)$ is said to be periodic of period T_k and order k if there exist nonnegative

integers $m \geq 0$ and $k \geq 1$ such that k is the smallest integer for which $z_m^+ = z_{m+k}^+$ and $T_k = \sum_{i=m}^{m+k-1} \Phi(z_i) = \sum_{i=m}^{m+k-1} s_i$.

For simplification, we denote a periodic trajectory of period T_k and order k by an order k periodic solution. An order k periodic solution is called an order k limit cycle if it is isolated. For more details of the concepts and properties of continuous dynamical systems and impulsive dynamical systems, see [12, 15, 17].

Lemma 3 (Analogue of Poincaré Criterion [10, 11]). *The T-periodic solution $(x, y) = (\xi(t), \eta(t))$ of system*

$$\begin{aligned} \frac{dx}{dt} &= P(x, y), \\ \frac{dy}{dt} &= Q(x, y), \end{aligned} \qquad \text{if } \phi(x, y) \neq 0,$$

$$\begin{aligned} \Delta x &= \alpha(x, y), \\ \Delta y &= \beta(x, y), \end{aligned} \qquad \text{if } \phi(x, y) = 0, \tag{6}$$

is orbitally asymptotically stable and enjoys the property of asymptotic phase if the Floquet multiplier μ_2 satisfies the condition $|\mu_2| < 1$, where

$$\mu_2 = \prod_{k=1}^{q} \Delta_k \cdot \exp\left(\int_0^T \left[\frac{\partial P}{\partial x}(\xi(t), \eta(t)) + \frac{\partial Q}{\partial y}(\xi(t), \eta(t)) \right] dt \right), \tag{7}$$

with

$$\Delta_k = \frac{P_+ \left((\partial\beta/\partial y)(\partial\phi/\partial x) - (\partial\beta/\partial x)(\partial\phi/\partial y) + \partial\phi/\partial x \right) + Q_+ \left((\partial\alpha/\partial x)(\partial\phi/\partial y) - (\partial\alpha/\partial y)(\partial\phi/\partial x) + \partial\phi/\partial y \right)}{P(\partial\phi/\partial x) + Q(\partial\phi/\partial y)}, \tag{8}$$

and P, Q, $\partial\alpha/\partial x$, $\partial\alpha/\partial y$, $\partial\beta/\partial x$, $\partial\beta/\partial y$, $\partial\phi/\partial x$, and $\partial\phi/\partial y$ are calculated at the point $(\xi(t_k), \eta(t_k))$, $P_+ = P(\xi(t_k^+), \eta(t_k^+))$ and $Q_+ = Q(\xi(t_k^+), \eta(t_k^+))$. Here $\phi(x, y)$ is a sufficiently smooth function such that $\operatorname{grad}\phi(x, y) \neq 0$, *and t_k ($k \in \mathbf{N}$) is the time of the kth jump.*

Since system (1) has been investigated by many scholars, bifurcations and phase portraits were also addressed in detail [2, 8, 9]. Here we briefly review the dynamics of system (1) which are useful in this study. The two isoclines of system (1) are denoted by L_1 and L_2, where $L_1 : u = I + v^2$, $L_2 : u = bv$. If we fix parameters a and b, choosing I as a variable, then the following results can be obtained easily.

Lemma 4 (see [2, 8, 9]). *(1) For $I > b^2/4$, there is no equilibrium in system (1). A saddle-node bifurcation curve is defined by $\{(b, I);\ I_{SN} = b^2/4\}$ ($(I, b) \in R^2$), and there is a unique equilibrium $E^*(v^*, u^*) = (b/2, b^2/2)$ for system (1).*

(2) For $I < b^2/4$, there are two equilibria $E_{1,2}(v_{1,2}, u_{1,2})$ for system (1); here $v_{1,2} = (b \pm \sqrt{b^2 - 4I})/2$, $u_{1,2} = (b^2 \pm b\sqrt{b^2 - 4I})/2$. An Andronov-Hopf bifurcation line is defined by $\{(b, I);\ b > a,\ I_{AH} = ab/2 - a^2/4\}$ ($(I, b) \in R^2$). A homoclinic bifurcation occurs on a curve approximated by $\{(b, I);\ b > a,\ I_{hom} = a^2/4 + a(b - a)/2 - 6(b - a)^2/25 + \mathcal{O}(|b - a|^3)\}$ ($(I, b) \in R^2$). Moreover, the curves I_{SN}, I_{AH}, and I_{hom} meet with common tangents at the codimension two Bogdanov-Takens bifurcation point ($b = a,\ I = a^2/4$).

Remark 5. From Lemma 4, model (1) could present six different qualitative dynamics when choosing I as a variable including the following:

(i) if $I < I_{\text{hom}}$, then the homoclinic orbit disappears and the stable and unstable manifolds separate to create an unbounded trapping region;

(ii) if $I = I_{\text{hom}}$, then there exists a homoclinic orbit;

(iii) if $I_{\text{hom}} < I < I_{\text{AH}}$, then there exists an unstable limit cycle;

(iv) if $I = I_{\text{AH}}$, then an Andronov-Hopf bifurcation occurs;

(v) if $I_{\text{AH}} < I < I_{\text{SN}}$, then E_2 is an unstable equilibrium point and E_1 is a saddle;

(vi) if $I = I_{\text{SN}}$, then E_1 (E_1 and E_2 coincide) is a saddle-node point; if $I > I_{\text{SN}}$, then there is no fixed point for system (1). Moreover, case (i) to case (v) are classified as the type 2 neurons, while case (vi) is corresponding to the type 1 neurons (for details see [9]).

In order to address the global dynamics of system (2), we consider case ($I = I_{\text{hom}}$) at which there exists a homoclinic orbit based on the qualitative behaviors of ODE model (1). In this case the system has two fixed points E_1 and E_2, and the solution initiating from the inside of the homoclinic orbit may not reach the threshold v_p under certain conditions (see more details later), which means that the impulsive effects may not happen. This indicates that system (2) may exhibit rich dynamics due to different values of the threshold and the dynamics presented in this case could be more complicated than other cases. Therefore, if we can investigate the global dynamics of this case in detail by using the theories of the ISDS and analytic techniques, then by using similar methods the dynamics of the remaining cases could be studied.

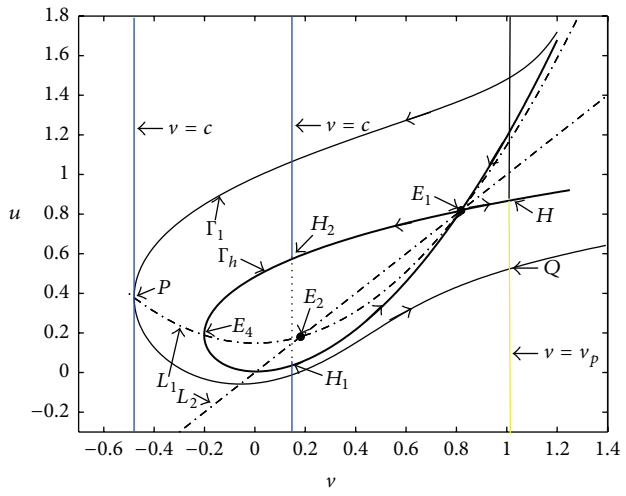

Figure 1: Illustrations of the domains of phase set and impulsive set for case (A_1). The blue lines represent the phase sets and the yellow line denotes the impulsive set.

3. Mathematical Analysis and Main Results

3.1. Impulsive Set and Phase Set. In order to investigate the existence of order k periodic solutions, the Poincaré map is constructed first. Nevertheless, it is essential to know that the exact conditions under which the solution of system (2) starting from $(v_0^+, u_0^+) \in \mathscr{P}$ is free from impulsive effects, that is to say, the more exact phase set $\mathscr{P}$, should be provided. Moreover, the impulsive set $\mathscr{I}$ defined in Section 2 is the maximum interval for the vertical coordinates. Therefore, the part of $\mathscr{I}$ which the solution of system (2) can not reach will be removed and then the exact domains of impulsive set can be obtained. From now on, unless otherwise specified we assume that $I = I_{\text{hom}}$ $(b > a)$ throughout the paper.

Based on different positions of v_p we consider the following three cases:

(A_1) $v_p \geq v_1$;
(A_2) $v_2 < v_p < v_1$;
(A_3) $v_p \leq v_2$.

The homoclinic cycle is denoted by Γ_h, and we let v_4 be the horizontal component of the small intersection point of the homoclinic cycle Γ_h with the line L_1 (denoted by $E_4 = (v_4, u_4)$; see Figure 1). For case (A_1), v_p intersects with the right branch of the homoclinic cycle at two points and we denote the lower point by $H(v_p, u_H)$. According to the relations among c, v_1, and v_4, there may be three cases for c: $c < v_4$, $v_4 \leq c \leq v_1$, or $c > v_1$. If $c < v_4$, then there exists a trajectory Γ_1 such that the line $v = c$ tangents to the curve Γ_1 at the point $P(c, u_P)$; here $u_P = I + c^2$. Clearly, the curve Γ_1 also intersects the line $v = v_p$ at two points and we denote the lower point by $Q(v_p, u_Q)$. Therefore, if $c < v_4$, then the impulsive set is defined by $\mathscr{I}_1 = \{(v, u) \in R^2 \mid v = v_p,\ -\infty \leq u \leq u_Q\}$ and the phase set is defined by $\mathscr{P}_1 = \{(v^+, u^+) \in R^2 \mid v^+ = c,\ u^+ \in D_1\}$; here $D_1 = [-\infty, u_Q + d]$. If so, any trajectory of system (2) initiating from the interior of the curve Γ_1 either cannot reach the impulsive set or reaches the interval $(u_Q, v_p^2 + I]$ and then maps to the phase set $\mathscr{P}_1$ after one time impulsive effect. If $v_4 \leq c \leq v_1$, then the line $v = c$ intersects the left branch of homoclinic cycle Γ_h at two points, denoted by $H_1 = (c, u_{H_1})$ and $H_2 = (c, u_{H_2})$. Thus, the impulsive set can be defined as $\mathscr{I}_2 = \{(v, u) \in R^2 \mid v = v_p,\ -\infty \leq u < u_H\}$ and the phase set is defined by $\mathscr{P}_2 = \{(v^+, u^+) \in R^2 \mid v^+ = c,\ u^+ \in D_2\}$; here $D_2 = \{(u_{H_2}, +\infty] \cup [-\infty, u_{H_1})\} \cap [-\infty, u_H + d)$. Moreover, the trajectories initiating from $(v^+, u^+) \in \mathscr{P}$ with $u_{H_1} \leq u^+ \leq u_{H_2}$ will be free from the impulsive effects and will tend to the stable equilibrium E_2. If $c > v_1$, then by using the same methods as subcase $c < v_4$ the impulsive set is defined by $\mathscr{I}_1$, and the phase set is defined by $\mathscr{P}_1$.

For case (A_2) (as shown in Figure 2(a)), that is, $v_2 < v_p < v_1$, there exists a curve Γ_2 which tangents to the line $v = v_p$ at a point $T = (v_p, v_p^2 + I)$. Besides, the curve Γ_2 must intersect the line L_1 at a point $E_3(v_3, v_3^2 + I)$ such that Γ_2 tangents to the line L_1 at this point. If $c \leq v_3$, then the curve Γ_1 which tangents to the line $v = c$ at the point P must intersect the line $v = v_p$ at two points; the lower intersect point is denoted by Q. Therefore, the impulsive set is defined by $\mathscr{I}_1$, and the phase set is defined by $\mathscr{P}_1$. If $c > v_3$, then the curve Γ_2 must intersect the line $v = c$ at two points, denoted by $P_1 = (c, u_{P_1})$ and $P_2 = (c, u_{P_2})$. Thus, the impulsive set can be defined as $\mathscr{I}$ and the phase set is defined by $\mathscr{P}_3 = \{(v^+, u^+) \in R^2 \mid v^+ = c,\ u^+ \in D_3\}$; here $D_3 = \{[u_{P_2}, +\infty] \cup [-\infty, u_{P_1}]\} \cap [-\infty, v_p^2 + I + d]$. Moreover, any trajectories initiating from $(v^+, u^+) \in \mathscr{P}$ with $u_{P_1} < u^+ < u_{P_2}$ will be free from the impulsive effects and will tend to the stable equilibrium E_2.

For case (A_3) (as shown in Figure 2(b)), by using the same methods as cases (A_1) and (A_2), the impulsive set and the phase set can be defined as $\mathscr{I}_1$ and $\mathscr{P}_1$, respectively.

In conclusion, we list all possible cases for the domains of impulsive sets and phase sets of model (2) in Table 1 based on the above analyses. It is found that the basic phase set $\mathscr{P}$ can not be used to define the real phase set of model (2) for any case, which indicates that the exact domains of phase set of model (2) should be carefully discussed before carrying out qualitative analyses.

Table 1: Exact domains of impulsive set and phase set of system (2).

Cases	$v = c$	Impulsive set	Phase set
(A_1)	$c < v_4, c > v_1$	$\mathscr{I}_1$	$\mathscr{P}_1$
	$v_4 \leq c \leq v_1$	$\mathscr{I}_2$	$\mathscr{P}_2$
(A_2)	$c \leq v_3$	$\mathscr{I}_1$	$\mathscr{P}_1$
	$c > v_3$	$\mathscr{I}$	$\mathscr{P}_3$
(A_3)	$c < v_2$	$\mathscr{I}_1$	$\mathscr{P}_1$

3.2. Poincaré Map. Assuming that any solution $\Pi_{z_0^+}$ with initial condition $z_0^+ = (v_0^+, u_0^+) \in \mathscr{P}_j$ $(j = 1, 2, 3)$ experiences impulses $k + 1$ times (finite or infinite), then the corresponding coordinates are denoted as $p_i = (v_p, u_i) \in \mathscr{I}_{j'}$ and $p_i^+ = (c, u_i^+) \in \mathscr{P}_j$, $i = 1, 2, \ldots, k$, $j' = 1, 2$; here the point p_i^+ is the impulsive point of p_i after one time impulsive

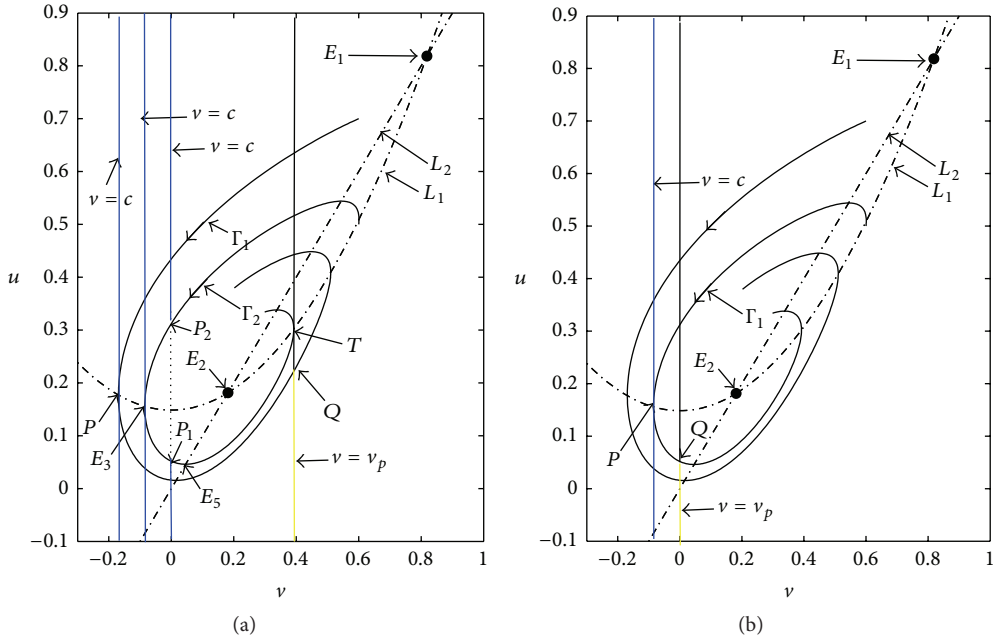

FIGURE 2: Illustrations of the domains of phase set and impulsive set: (a) for case (A_2); (b) for case (A_3).

effect. Therefore, if both points p_i^+ and p_{i+1} lie in the same trajectory Γ for $i = 1, 2, \ldots, k$, then the point p_{i+1} is only determined by p_i^+; that is, u_{i+1} can be only determined by u_i^+, which can be expressed by $u_{i+1} = g(u_i^+)$. Clearly, function g is continuously differentiable according to the theorem of Cauchy-Lipschitz with parameters.

In order to provide the exact domains of the Poincaré map, we first need to know under what conditions the trajectory initiating from $p_i^+ \in \mathscr{P}_j$ can not reach the impulsive set. From the analysis of Section 3.1, there may be two possible cases.

Case 1. The first case is $v_p \geq v_1$ and $v_4 \leq c \leq v_1$.

Case 2. The second case is $v_2 < v_p < v_1$ and $c > v_3$.

For Case 1, it follows from Section 3.1 that if the initial point p_i^+ lies on the homoclinic cycle Γ_h or its interior, then the trajectory can not reach the line $v = v_p$ forever, which indicates that this trajectory is free from impulsive effects, as shown in Figure 1, so we need $p_i^+ \in \mathscr{P}_2$. For Case 2, if the initial point p_i^+ lies in the interior of the curve Γ_2, then the trajectory can not reach the line $v = v_p$ and will tend to the stable equilibrium E_2, which means that this trajectory is also free from impulsive effects, and then we need $p_i^+ \in \mathscr{P}_3$, as shown in Figure 2(b).

In addition to the above two cases, any trajectory of system (2) initiating from $p_i^+ \in \mathscr{P}_j$ can reach at the point $p_{i+1} \in \mathscr{S}$. Due to the impulsive effects, we have

$$u_{i+1}^+ = g\left(u_i^+\right) + d \triangleq \varphi\left(u_i^+\right), \quad i = 1, 2, \ldots, k. \tag{9}$$

To explore the dynamical behaviors of system (2), the Poincaré map is constructed in the exact domains of the phase set.

Lemma 6 (see [18]). *The Poincaré map for the impulsive points of model (2) defined in phase set can be defined as*

(A_1)

$$u_{i+1}^+ = \begin{cases} \varphi\left(u_i^+\right),\ u_i^+ \in D_1 & \text{if } c < v_4,\ c > v_1, \\ \varphi\left(u_i^+\right),\ u_i^+ \in D_2 & \text{if } v_4 \leq c \leq c_1, \end{cases} \tag{10}$$

(A_2)

$$u_{i+1}^+ = \begin{cases} \varphi\left(u_i^+\right),\ u_i^+ \in D_1 & \text{if } c \leq v_3, \\ \varphi\left(u_i^+\right),\ u_i^+ \in D_3 & \text{if } c > v_3, \end{cases} \tag{11}$$

(A_3)

$$u_{i+1}^+ = \varphi\left(u_i^+\right),\ u_i^+ \in D_1 \text{ if } c < v_2, \tag{12}$$

where the Poincaré map $\varphi(u_i^+)$ is defined by (9).

Since the function g and consequently the function φ are continuously differentiable with respect to u_i^+, for each fixed point of Poincaré map φ, there exists an associated periodic solution for system (2).

3.3. Existence and Stability of Order 1 Periodic Solution. In this subsection, we mainly focus on investigating the existence and stability of an order 1 periodic solution of system (2) based on cases (A_1), (A_2), and (A_3), which could be realized by studying the existence and stability of the fixed point of the Poincaré map. To this end, we have following main results.

Theorem 7. *If $c < v_4$ or $c > v_1$ for case (A_1) (or if $c \leq v_3$ for case (A_2) or if $c < v_2$ for case (A_3)), then the fixed point of the*

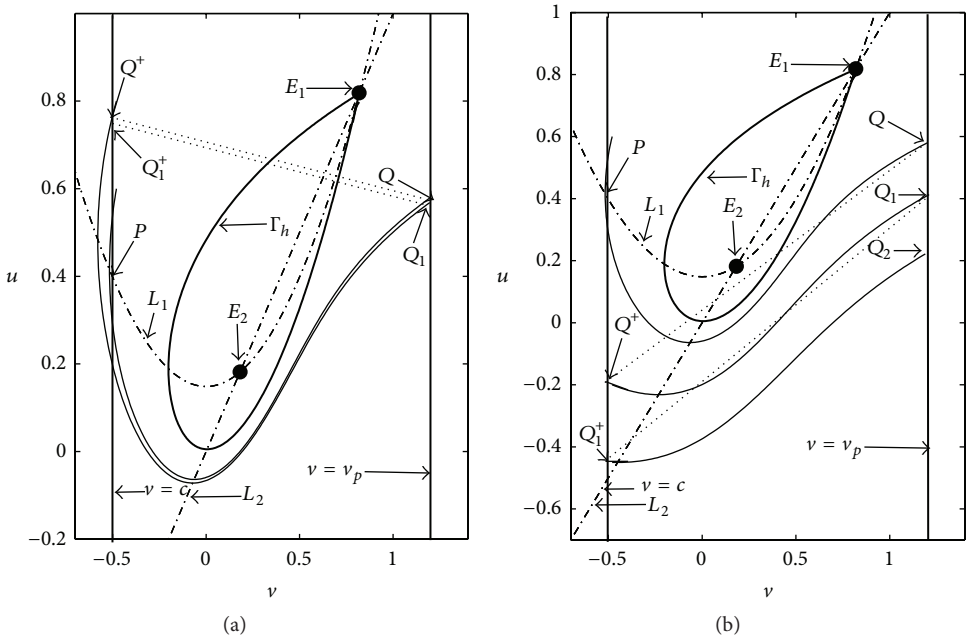

FIGURE 3: Location of the periodic solution of system (2) for case (A_1) when $c < v_4$ or $c > v_1$. (a) The case when the pulsed point Q^+ is above the point P; (b) the case when the pulsed point Q^+ lies below the point P.

Poincaré map φ exists and consequently there exists an order 1 periodic solution for system (2).

Proof. Firstly, we prove that there exists a fixed point for the Poincaré map φ if $c < v_4$ or $c > v_1$ for case (A_1). Then by using the same methods, it can be demonstrated that the results are also true for case (A_2) when $c \le v_3$ or for case (A_3) when $c < v_2$.

For the first case, the curve Γ_1 initiating from the point $P(c, u_P)$ tangents to the line $v = c$ and reaches the line $v = v_p$ at the point $Q(v_p, u_Q)$ (clearly, $u_Q = g(u_P)$), and then the point Q maps to the point $Q^+(c, u_Q + d)$ (or $Q^+(c, u_{Q^+})$) due to the impulsive effect. To determine the location of the point Q^+, we assume that there exists d_0 such that $u_Q + d_0 = I + c^2$; then the point Q^+ coincides with the point P for $d = d_0$. Obviously, the Poincaré map φ has a fixed point and consequently the curve $\widehat{PQ}$ forms an order 1 periodic solution for system (2).

If $d > d_0$ (see Figure 3(a)), then the pulsed point Q^+ is above the point P. Thus, the following inequality holds:

$$\varphi\left(u_P\right) - u_P = u_{Q^+} - u_P > 0. \tag{13}$$

Furthermore, the trajectory initiating from the point Q^+ will meet the line v_p at a point, denoted by $Q_1(v_p, g(u_{Q^+}))$. In view of disjointness of any two trajectories, the point Q_1 lies below the point Q. Then the point Q_1 maps to the point $Q_1^+(c, u_{Q_1^+})$ after one time impulsive effect. Besides, the two line segments $\overline{QQ^+}$ and $\overline{Q_1Q_1^+}$ satisfy $\overline{QQ^+} \parallel \overline{Q_1Q_1^+}$, which indicates that the point Q_1^+ must lie below the point Q^+. So another inequality holds:

$$\varphi\left(u_{Q^+}\right) - u_{Q^+} = u_{Q_1^+} - u_{Q^+} < 0. \tag{14}$$

It follows from (13) and (14) that the Poincaré map has a fixed point, which corresponds to an order 1 periodic solution of system (2).

If $d < d_0$, then the pulsed point Q^+ lies below the point P (see Figure 3(b)). Thus, the trajectory starting from the point Q^+ will reach the line $v = v_p$ at the point Q_1, and it is easy to see that the point Q_1 lies below the point Q because of the uniqueness of solutions. Then the point Q_1 maps to the point Q_1^+ after one time impulsive effect, where the point Q_1^+ lies below the point Q^+. By induction, it is noted that the point Q_{i+1}^+ lies below the point Q_i^+, $i = 1, 2, \ldots, n$, which indicates that the impulsive point series Q_i^+ is monotonically decreasing. That is,

$$\begin{aligned} -\infty \le u_{Q_n^+} < \cdots < u_{Q_i^+} < \cdots < u_{Q_1^+} < u_{Q^+} < u_p \\ = I + c^2. \end{aligned} \tag{15}$$

Therefore, what we want to show in the following is that the impulsive point series $u_{Q_i^+}$ is bounded. First of all, $dv/dt > 0$ for $v \in [c, v_p]$; that is to say, v is monotonically increasing with respect to t. This indicates that any solution initiating from $z_0^+ = (v_0^+, u_0^+) \in \mathscr{P}_1$ with $c \le v_0^+ \le v_p$ satisfies $c \le v(t) \le v_p$. From the second equation of system (1) we have

$$a\left(bc - u\left(t\right)\right) \le \frac{du\left(t\right)}{dt} \le a\left(bv_p - u\left(t\right)\right). \tag{16}$$

According to Comparison Theorem of ODE [19] we can get

$$\begin{aligned} bc + \exp\left(-at\right)\left(u_0^+ - bc\right) \\ \le u\left(t\right) \le bv_p + \exp\left(-at\right)\left(u_0^+ - bv_p\right). \end{aligned} \tag{17}$$

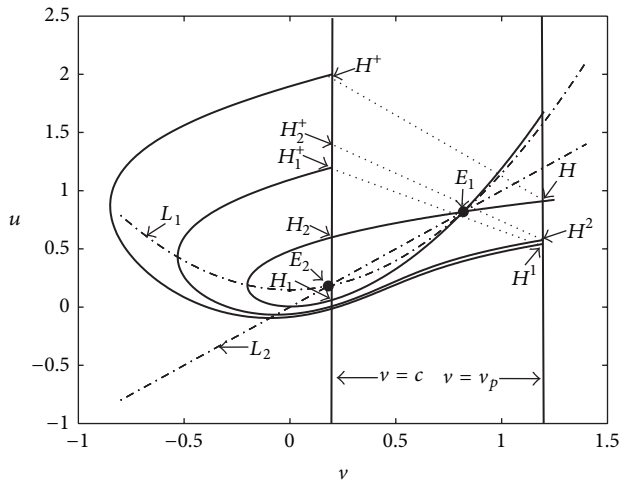

Figure 4: Location of the periodic solution of system (2) for case (A_1) when $v_4 \le c \le v_1$.

According to (17), it is known that the pulsed sequence $u_{Q_i^+}$ (or Poincaré map) is bounded and monotonically decreasing. This indicates that the sequence $u_{Q_i^+}$ has a limit point. Therefore, the Poincaré map has a fixed point when $c < v_4$ or $c > v_1$ for case (A_1), which corresponds to an order 1 periodic solution of system (2). This completes the proof. □

Remark 8. For case (A_1) when $c > v_1$, there exists a unique homoclinic cycle in system (2). In particular, there exists d^* such that the point H maps to the point H_{ru} which lies on the stable manifold of the right branch of homoclinic cycle Γ_h in the phase set; it is easy to see that the curve $\widehat{H_{ru}E_1H}$ forms a unique homoclinic cycle with impulsive effects. Moreover, if $d > d^*$ or $d < d^*$, then the homoclinic cycle is broken and an order 1 periodic solution is generated for system (2).

Theorem 9. *If $v_4 \le c \le v_1$ and $u_{H_1^+} > u_{H_2}$ for case (A_1) where $u_{H_1^+}$ is the vertical coordinate of the initial point (c, u_{H_2}) from which the solution experiences two time impulsive effects, then there exists a fixed point for the Poincaré map φ which corresponds to an order 1 periodic solution for system (2).*

Proof. For this case (as shown in Figure 4), the line $v = c$ intersects the left branch of homoclinic cycle Γ_h at two points $H_1 = (c, u_{H_1})$ and $H_2 = (c, u_{H_2})$. In the region above the line L_2, we have $du(t)/dt < 0$; that is to say, the adaptation variable $u(t)$ is decreasing in this area. While in the region lying below the line L_2 one has $du(t)/dt > 0$, this indicates that the adaptation variable $u(t)$ is increasing. Therefore, the following inequality must hold true:

$$u_{H_1} < u_{H_2} < u_1 < u_H. \tag{18}$$

Due to impulsive effects, the point H maps to the point H^+ which is above the point H_2 due to $d > 0$ and $u_H > u_{H_2}$. Thus, the trajectory initiating from the point H^+ will meet the line v_p at two points, the lower point denoted by $H^1(v_p, u_{H^1})$. The point H^1 must lie below the point H in view of disjointness of any two trajectories. Then the point H^1 maps to the point $H_1^+(c, u_{H_1^+})$ after one time impulsive effect. For the location of the point H_1^+, it follows from the assumption that the point H_1^+ must lie above the point H_2 and lies below the point H^+. Thus, we have following inequality:

$$\varphi(u_{H^+}) - u_{H^+} = u_{H_1^+} - u_{H^+} < 0. \tag{19}$$

Similarly, the solution starting from the point H_1^+ meets the line $v = v_p$ at the point H^2 which lies between H and H^1, and then H^2 maps to the point H_2^+ which lies between H^+ and H_1^+. Thus, the following inequality holds:

$$\varphi\left(u_{H_1^+}\right) - u_{H_1^+} = u_{H_2^+} - u_{H_1^+} > 0. \tag{20}$$

It follows from (19) and (20) that there exists a fixed point for the Poincaré map, which is also an order 1 periodic solution of system (2). This completes the proof. □

Theorem 10. *If $c > v_3$, $u_{T^+} \ge u_{P_2}$, and $u_{T_1^+} \ge u_{P_2}$ (or $u_{T^+} \le u_{P_1}$) for case (A_2) where u_{T^+} is the vertical coordinate of the initial point (c, u_{P_2}) from which the solution experiences one time impulsive effect whilst $u_{T_1^+}$ is the vertical coordinate of the initial point (c, u_{P_2}) from which the solution experiences two time impulsive effects, then the fixed point of the Poincaré map φ exists and consequently there exists an order 1 periodic solution for system (2).*

Proof. Assuming that the first intersection point of the line L_2 with the curve Γ_2 (initiating from the point P_2) is denoted as $E_5(v_5, u_5)$, see Figure 2(a). Hence, if $c \ge v_5$, then the point T is above the point P_1 because the adaptation variable $u(t)$ is increasing in the region that lies below the line L_2. Further, the pulsed point T^+ is above the point P_1 after one time impulsive effect due to $d > 0$. Therefore, if $u_{T^+} \ge u_{P_2}$ and $u_{T_1^+} \ge u_{P_2}$, then, by using the same method as the proof of Theorem 9, it can be proved that there exists a fixed point for the Poincaré map φ.

If $v_3 < c < v_5$, then there are two possible cases for the relations of u_{P_1} and u_T: $u_T > u_{P_1}$ or $u_T \le u_{P_1}$. For the former, it is clear that the point T is still above the point P_1. From the above analysis, there exists a fixed point for the Poincaré map. For the latter, if $u_{T^+} \ge u_{P_2}$ and $u_{T_1^+} \ge u_{P_2}$, then there exists a fixed point for the Poincaré map; if $u_{T^+} \le u_{P_1}$, then, by using the same analytic techniques as shown in Theorem 7 for the case $d \le d_0$, it can be shown that there exists a fixed point for the Poincaré map φ, which means that system (2) has an order 1 periodic solution. This completes the proof. □

Remark 11. If $c > v_3$ and $u_{P_1} < u_{T^+} < u_{P_2}$ for case (A_2), then any solution initiating from $(c, u_0^+) \in \mathscr{P}_3$ experiences finite pulses and then tends to the stable equilibrium E_2, which is known as phasic spiking mode [2].

To sum up, the conditions for the existence of an order 1 periodic solution of system (2) are provided for cases (A_1), (A_2), and (A_3). In addition, parameter sets which guarantee the existence of a unique homoclinic cycle and phasic spiking are also obtained. Furthermore, in the following the stability of the order 1 periodic solution will be investigated by using

the Analogue of Poincaré Criterion which is introduced in Section 2.

Theorem 12. *The order 1 periodic solution $(v,u) = (\xi(t),\eta(t))$ of system (2) is orbitally asymptotically stable and enjoys the property of asymptotic phase if*

$$\left|\frac{I + c^2 - (\eta_0 + d)}{I + v_p^2 - \eta_0} \exp\left(\int_0^T G(t)\,dt\right)\right| < 1 \tag{21}$$

with $G(t) = 2\xi(t) - a$.

Proof. We first show that the order 1 periodic solution which is obtained in Theorem 7 is orbitally asymptotically stable. To show this, assume that the order 1 periodic solution with period T passes through the points $E(v_p,\eta_0)$ and $E^+(c,\eta_0+d)$. Note that the explicit expression and period T of the order 1 periodic solution are unknown. Thus, Lemma 3 provides a necessary tool to discuss stability of this periodic solution. To do this, we denote

$$\begin{aligned} P(v,u) &\doteq I + v^2 - u,\\ Q(v,u) &\doteq a(bv - u),\\ \alpha(v,u) &= c - v,\\ \beta(v,u) &= d,\\ \phi(v,u) &= v - v_p,\\ (\xi(T),\eta(T)) &= (v_p,\eta_0),\\ (\xi(T^+),\eta(T^+)) &= (c,\eta_0 + d). \end{aligned} \tag{22}$$

Then

$$\begin{aligned} &\frac{\partial P}{\partial v} = 2v,\\ &\frac{\partial Q}{\partial u} = -a,\\ &\frac{\partial \alpha}{\partial v} = -1,\\ &\frac{\partial \alpha}{\partial u} = \frac{\partial \beta}{\partial v} = \frac{\partial \beta}{\partial u} = \frac{\partial \phi}{\partial u} = 0,\\ &\frac{\partial \phi}{\partial v} = 1,\\ &\Delta_1 = \frac{P_+\left((\partial\beta/\partial u)(\partial\phi/\partial v) - (\partial\beta/\partial v)(\partial\phi/\partial u) + \partial\phi/\partial v\right) + Q_+\left((\partial\alpha/\partial v)(\partial\phi/\partial u) - (\partial\alpha/\partial u)(\partial\phi/\partial v) + \partial\phi/\partial u\right)}{P(\partial\phi/\partial v) + Q(\partial\phi/\partial u)}\\ &\quad = \frac{P^+(\xi(T^+),\eta(T^+))}{P(\xi(T),\eta(T))} = \frac{I + c^2 - (\eta_0 + d)}{I + v_p^2 - \eta_0}. \end{aligned} \tag{23}$$

Moreover, we have

$$\begin{aligned} &\exp\left(\int_0^T \left[\frac{\partial P}{\partial v}(\xi(t),\eta(t)) + \frac{\partial Q}{\partial u}(\xi(t),\eta(t))\right] dt\right)\\ &\quad = \exp\left(\int_0^T [2\xi(t) - a]\,dt\right) = \exp\left(\int_0^T G(t)\,dt\right). \end{aligned} \tag{24}$$

Therefore,

$$\begin{aligned} \mu_2 &= \Delta_1\\ &\cdot \exp\left(\int_0^T \left[\frac{\partial P}{\partial x}(\xi(t),\eta(t)) + \frac{\partial Q}{\partial y}(\xi(t),\eta(t))\right] dt\right)\\ &= \frac{I + c^2 - (\eta_0 + d)}{I + v_p^2 - \eta_0} \exp\left(\int_0^T G(t)\,dt\right). \end{aligned} \tag{25}$$

From the proof of Theorem 7, there exists d_0 such that the point Q^+ coincides with the point P when d_0 satisfies $u_Q + d_0 = I + c^2$. Hence, $|\mu_2| = 0 < 1$ leads to the fact that the order 1 periodic solution is orbitally asymptotically stable.

For $d < d_0$, then the point Q^+ lies below the point P. Obviously, the point E^+ lies below the point P; that is, $I + c^2 > \eta_0 + d$. It follows from $\exp(\int_0^T G(t)dt) > 0$ and $I + v_p^2 - \eta_0 > 0$ that $\mu_2 > 0$ for $d < d_0$. For $d > d_0$, one can get $\mu_2 < 0$.

Therefore, if $|\mu_2| < 1$, that is, inequality (21) holds true, then the order 1 periodic solution $(\xi(t),\eta(t))$ is orbitally asymptotically stable and enjoys the property of asymptotic phase. Similarly, we can prove that the order 1 periodic solution $(\xi(t),\eta(t))$ obtained from Theorems 9 and 10 is orbitally asymptotically stable as well. This completes the proof. □

3.4. Existence and Nonexistence of Order k Periodic Solutions. Our main purpose in this subsection is to study the existence and nonexistence of order k ($k \geq 2$) periodic solutions of system (2).

Theorem 13. *Assume that $c < v_4$ or $c > v_1$ for case (A_1) (or $c \le v_3$ for case (A_2) or $c < v_2$ for case (A_3)); if $u_Q^+ < I + c^2$, then system (2) does not have an order k $(k \ge 2)$ periodic solution other than an order 1 periodic solution.*

Proof. If $u_Q^+ < I + c^2$, then all the impulsive points initiating from phase set $\mathscr{P}_1$ lie below the point P. From the proof of Theorem 7, the impulsive point series Q_i^+ satisfies (15). Besides, the pulsed segments $\overline{QQ^+}, \overline{Q_1Q_1^+}, \ldots, \overline{Q_nQ_n^+}$ are parallel, that is,

$$\overline{QQ^+} \parallel \overline{Q_1Q_1^+} \parallel \cdots \parallel \overline{Q_nQ_n^+}. \tag{26}$$

It follows from (15) that an order k $(k \ge 2)$ periodic solution does not exist for system (2). This completes the proof. □

Theorem 14. *If $v_4 \le c \le v_1$ and $u_{H_1^+} > u_{H_2}$ for case (A_1), then system (2) does not have an order k $(k \ge 3)$ periodic solution other than the order 1 and order 2 periodic solutions.*

Proof. If $u_{H_1^+} > u_{H_2}$, then all the impulsive points initiating from $(u_{H_2}, u_{H^+}] \subset \mathscr{P}_1$ are above the point H_2. From the proof of Theorem 9, it is easy to get $u_{H_2} < u_{H_1^+} < u_H^+$ and $u_{H_2} < u_{H_2^+} < u_H^+$. Assume that the trajectory of system (2) with initial value (c, u_H^+) experiences k times impulsive effects, and for the relations of $u_{H_i^+}$ we have the following two possibilities ($i = 1, 2, \ldots, k$; without loss of generality, we assume that there exists a positive integer n such that $k = 2n + 1$):

(a) $u_{H_2} < \cdots < u_{H_{2n}}^+ < u_{H_{2(n-1)}}^+ < \cdots < u_{H_4}^+ < u_{H_2}^+ < u_H^+$,

(b) $u_{H_2} < u_{H_1^+} < u_{H_3^+} < u_{H_5^+} < \cdots < u_{H_{2n-1}}^+ < u_{H_{2n+1}}^+ < \cdots < u_H^+$.

From (a) and (b), we conclude that the impulsive point series $\{u_{H_{2n}}^+\}$ is decreasing in the interval $(u_{H_2}, u_{H^+}]$ and $\{u_{H_{2n+1}}^+\}$ is increasing in the interval $(u_{H_2}, u_{H^+}]$, and they both converge to a fixed point in this bounded region. Moreover, note that all the impulsive lines are parallel. Therefore, the Poincaré map φ has either a fixed point or a period two-point cycle; that is to say, system (2) does not have an order k $(k \ge 3)$ periodic solution if $u_{H_1^+} > u_{H_2}$. This completes the proof. □

From Theorem 14, the conditions for the nonexistence of an order k $(k \ge 3)$ periodic solution are provided for case (A_1) if $v_4 \le c \le v_1$ and $u_{H_1^+} > u_{H_2}$. By using the same methods, it is also confirmed that system (2) does not have an order k $(k \ge 3)$ periodic solution for another three cases: case (A_1) with $c < v_4$ (or $c > v_1$) and $u_{Q_1}^+ \ge I + c^2$; case (A_2) with $c \le v_3$ and $u_{Q_1}^+ \ge I + c^2$ (or with $c > v_3$ and $u_{T_1^+} \ge u_{P_2}$); case (A_3) with $c < v_2$ and $u_{Q_1}^+ \ge I + c^2$.

Assuming that any solution $\Pi_{z_{0^+}}$ with initial condition $z_0^+ = (c, u_0^+)$ (where $u_0^+ \in (-\infty, I + c^2)$, or $u_0^+ \in (-\infty, u_{H_1})$, or $u_0^+ \in (-\infty, u_{P_1})$) experiences k times impulsive effects (finite or infinite), we denote the corresponding coordinates $p_i^+ = (c, u_i^+)$, $i = 0, 1, 2, \ldots, k$. If $u_k^+ \le I + c^2$, it follows from $du(t)/dt > 0$ and $d > 0$ that the impulsive point sequence u_i^+ is increasing, and then we have

$$u_0^+ < u_1^+ < \cdots < u_k^+ \le I + c^2. \tag{27}$$

Further, if $k \to \infty$, then, by using the same methods as those shown in Theorem 13, there is no order k $(k \ge 2)$ periodic solution other than an order 1 periodic solution in system (2).

However, if there exists $j < k$ such that $u_{j-1}^+ \le I + c^2$ and $u_j^+ > I + c^2$, then we cannot determine the accurate position of u_{j+1}^+, which indicates that we can not determine the nonexistence of order k $(k \ge 3)$ periodic solution in this case. In fact, the kinetic behaviors of system (2) displayed in this case are very complicated and it is difficult to address the qualitative behaviors analytically. Nevertheless, a traditional approach to gain preliminary insight into the properties of a dynamic system is to carry out a one-dimensional bifurcation analysis. One-dimensional bifurcation diagrams show the dependence of the dynamic behaviors on a certain parameter. Therefore, we resort to numerical investigations to show what dynamics will be presented in system (2). To show this, we set the threshold $v_p = 3$ and fix all parameters from [8] as follows: $I_{\text{hom}} = 0.1485$, $a = 0.5$, $b = 1$, and $c = 2.5$ and then choosing d as a bifurcation parameter.

Figure 5 illustrates the bifurcation diagrams for system (2) with d as the control parameter. Figure 5(b) is the magnified part of Figure 5(a). For parameter $d > 5.93$, a stable order 1 periodic solution is observed. As parameter d is reduced, the order 1 periodic solution loses its stability and then there exists an order 2 periodic solution for system (2) via a period-doubling bifurcation. As d further decreased about $d \approx 3$, it can be seen that system (2) exhibits transitions from order n periodic solutions to order $(n + 1)$ periodic solutions $(n = 2, 3, 4, 5)$ via period-adding bifurcations involving chaotic bands. When parameter d is slightly less than 1.182, the periodic attractor suddenly disappears and the chaotic attractor abruptly appears, thus constituting a type of attractor crisis (the phenomenon of crisis shows that chaotic attractors can suddenly appear or disappear or change size discontinuously as a parameter smoothly varies [20]) (Figure 6). When $1.145 < d < 1.182$, the dynamics presented in model (2) is very complicated, including chaotic bands, periodic windows, period-double bifurcations, and period-halving bifurcations (for details see Figure 5(b)). With further reduction of d, period-halving bifurcations lead system (2) into a stable state of an order 1 periodic solution.

4. Conclusion

The quadratic integrate-and-fire model with a recovery variable has been recently used in very large-scale simulations of neural networks; it is stressed that this simple model is capable of reproducing the rich behavior of biological neurons, such as spiking, bursting, and mixed mode firing patterns and continuous spiking with frequency adaptation [1]. Consequently, mathematical analysis of the model not only has important theoretical significance, but also has direct

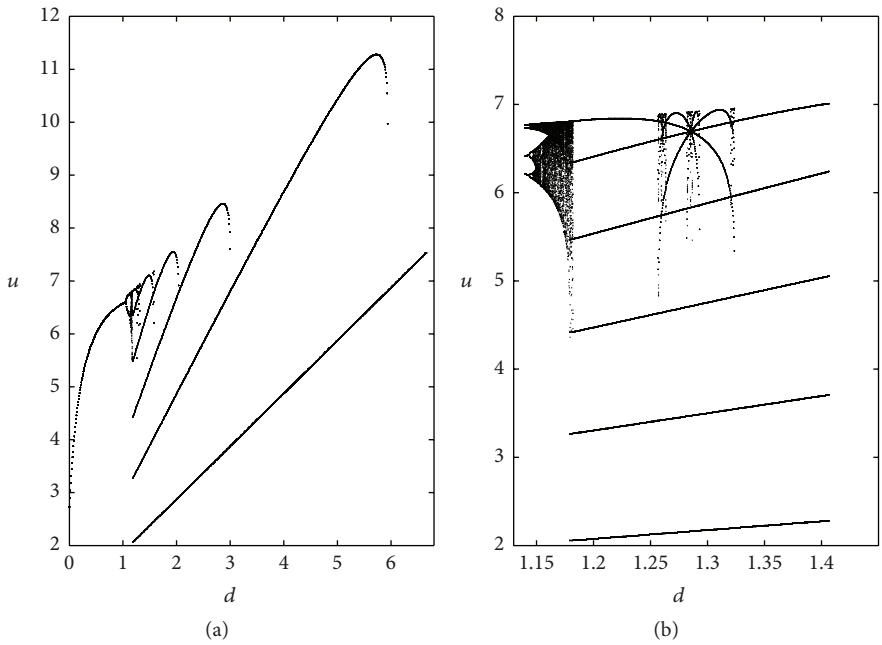

FIGURE 5: (a) Bifurcation diagram of the adaptation variable of system (2) with $I_{\text{hom}} = 0.1485$, $a = 0.5$, $b = 1$, $c = 2.5$, $v_p = 3$, and $d \in [0, 6.66]$. (b) The magnified part of (a).

biological relevance. Recently, the firing rates for fixed values of the recovery variable were studied by Shlizerman and Holmes [8]. Then the subthreshold dynamics were discussed in detail by Touboul [21]. Subsequently, the patterns of spikes were addressed numerically when the adaptation variable blows up [2, 22]. Here the main purpose is to provide a comprehensively qualitative analysis for all possible dynamics on whole parameter space for system (2) by using the theories of impulsive semidynamic system, and those theories have been applied broadly in many fields; for details see [23–27].

This paper mainly focuses on the most complex case $I = I_{\text{hom}}$ since other cases are easier and can be studied analogously. First of all, the impulsive and phase sets are defined exactly in line with the phase portraits of model (1), and then the Poincaré map is constructed in the exact phase sets. Further, the different parameter spaces for the existence and stability of order 1 periodic solution are investigated in detail by using the Poincaré map and the Analogue of Poincaré Criterion. In addition, the conditions for the homoclinic cycle with impulsive effects and phasic spiking are provided. Moreover, the existence and nonexistence of order k ($k \geq 2$) periodic solution are studied theoretically and numerically.

The Poincaré map has been constructed to investigate the existence of periodic solutions in neuron model, which allow us to better understand the working mechanism of the brain. The conditions for the regular spiking, bursting, and phasic spiking are provided; as regular spiking corresponds to an order 1 periodic solution and bursting corresponds to an order k ($k \geq 2$) periodic solution, this indicates that the parameters should be chosen carefully in order to control the number of spikes per burst. When an order 1 periodic solution loses its stability, model (2) exhibits very intricate dynamics, such as periodic windows, chaotic bands, period-doubling bifurcations, period-adding bifurcations, and period-halving bifurcations (for details see Figure 5). Particularly, it is noted that chaos whose electrophysiological signature is bursting has been observed in the simple neuron model as well as real neurons in vitro [28–33]. The results imply that the analytical methods can be used as the basis for understanding dynamical behaviors of neuron models.

To provide a more comprehensive theoretical analysis for system (2), the dynamics presented in the remaining cases will be studied in the future. Recently, with the aim of improving the effective simulation studies, an alternative has been made to develop minimal models of spiking neurons which reduced the dimensionality of variable space [34]. To this end, piecewise linear planar neuron models, which are described by a nonsmooth dynamical system, are a good choice and have become one of the most popular topics [34–37]. Therefore, these will be the main focus of our future research. It is hoped that such research, planned for the near future and to be reported elsewhere, will be useful for computational neuroscience.

Conflict of Interests

The authors declare that there is no conflict of interests regarding the publication of this paper.

Acknowledgments

This work was supported by the Fundamental Research Funds for the Central Universities (GK201305010,

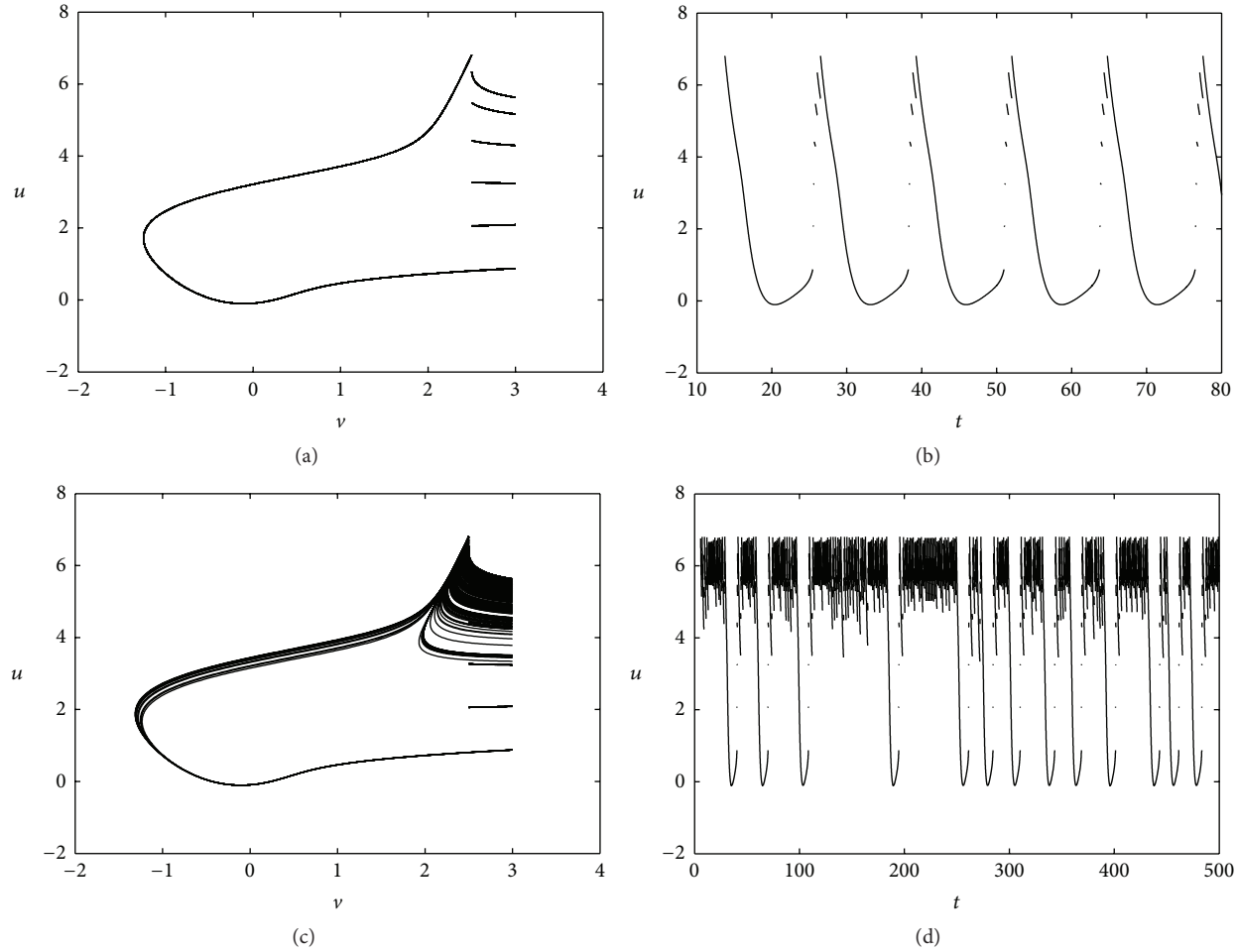

FIGURE 6: Attractor crisis of system (2) with parameters $I_{\text{hom}} = 0.1485$, $a = 0.5$, $b = 1$, $c = 2.5$, and $v_p = 3$. (a-b) Phase space projection and time series of an order 6 periodic solution for $d = 1.183$; (c-d) phase space projection and time series of a chaotic attractor for $d = 1.182$.

GK201401004) and by the National Natural Science Foundation of China (NSFC, 11171199, 11371030, and 11301320).

References

[1] E. M. Izhikevich, "Simple model of spiking neurons," *IEEE Transactions on Neural Networks*, vol. 14, no. 6, pp. 1569–1572, 2003.

[2] J. Touboul and R. Brette, "Spiking dynamics of bidimensional integrate-and-fire neurons," *SIAM Journal on Applied Dynamical Systems*, vol. 8, no. 4, pp. 1462–1506, 2009.

[3] R. FitzHugh, "Impulses and physiological states in theoretical models of nerve membrane," *Biophysical Journal*, vol. 1, no. 6, pp. 445–466, 1961.

[4] J. Nagumo, S. Arimoto, and S. Yoshizawa, "An active pulse transmission line simulating nerve axon," *Proceedings of the IRE*, vol. 50, no. 10, pp. 2061–2070, 1962.

[5] R. Brette and W. Gerstner, "Adaptive exponential integrate-and-fire model as an effective description of neuronal activity," *Journal of Neurophysiology*, vol. 94, no. 5, pp. 3637–3642, 2005.

[6] E. M. Izhikevich, "Which model to use for cortical spiking neurons?" *IEEE Transactions on Neural Networks*, vol. 15, no. 5, pp. 1063–1070, 2004.

[7] E. M. Izhikevich and G. M. Edelman, "Large-scale model of mammalian thalamocortical systems," *Proceedings of the National Academy of Sciences of the United States of America*, vol. 105, no. 9, pp. 3593–3598, 2008.

[8] E. Shlizerman and P. Holmes, "Neural dynamics, bifurcations, and firing rates in a quadratic integrate-and-fire model with a recovery variable. I: deterministic behavior," *Neural Computation*, vol. 24, no. 8, pp. 2078–2118, 2012.

[9] E. M. Izhikevich, *Dynamical Systems in Neuroscience: The Geometry of Excita*, MIT Press, Cambridge, Mass, USA, 2007.

[10] P. S. Simeonov and D. D. Bainov, "Orbital stability of periodic solutions of autonomous systems with impulse effect," *International Journal of Systems Science*, vol. 19, no. 12, pp. 2561–2585, 1988.

[11] D. D. Bainov and P. S. Simeonov, *Impulsive Differential Equations: Periodic Solutions and Applications*, Longman Scientific & Technical, 1993.

[12] K. Ciesielski, "On semicontinuity in impulsive dynamical systems," *Bulletin of the Polish Academy of Sciences. Mathematics*, vol. 52, no. 1, pp. 71–80, 2004.

[13] K. Ciesielski, "On stability in impulsive dynamical systems," *Bulletin of the Polish Academy of Sciences. Mathematics*, vol. 52, no. 1, pp. 81–91, 2004.

[14] K. Ciesielski, "On time reparametrizations and isomorphisms of impulsive dynamical systems," *Annales Polonici Mathematici*, vol. 84, no. 1, pp. 1–25, 2004.

[15] S. K. Kaul, "On impulsive semidynamical systems," *Journal of Mathematical Analysis and Applications*, vol. 150, no. 1, pp. 120–128, 1990.

[16] S. K. Kaul, "On impulsive semidynamical systems III: lyapunov stability," *Recent Trends in Differential Equations*, vol. 1, pp. 335–345, 1992.

[17] A. S. Matveev and A. V. Savkin, *Qualitative Theory of Hybrid Dynamical Systems*, Cambridge University Press, Cambridge, UK, 2000.

[18] L. N. Qian, Q. S. Lu, Q. G. Meng, and Z. S. Feng, "Dynamical behaviors of a prey–predator system with impulsive control," *Journal of Mathematical Analysis and Applications*, vol. 363, no. 1, pp. 345–356, 2010.

[19] E. A. Coddington and N. Levinson, *Theory of Ordinary Differential Equations*, Tata McGraw-Hill, 1955.

[20] C. Grebogi, E. Ott, and J. A. Yorke, "Crises, sudden changes in chaotic attractors, and transient chaos," *Physica D: Nonlinear Phenomena*, vol. 7, no. 1–3, pp. 181–200, 1983.

[21] J. Touboul and R. Brette, "Dynamics and bifurcations of the adaptive exponential integrate-and-fire model," *Biological Cybernetics*, vol. 99, no. 4-5, pp. 319–334, 2008.

[22] R. Naud, N. Marcille, C. Clopath, and W. Gerstner, "Firing patterns in the adaptive exponential integrate-and-fire model," *Biological Cybernetics*, vol. 99, no. 4-5, pp. 335–347, 2008.

[23] S. Y. Tang and R. A. Cheke, "State-dependent impulsive models of integrated pest management (IPM) strategies and their dynamic consequences," *Journal of Mathematical Biology*, vol. 50, no. 3, pp. 257–292, 2005.

[24] S. Y. Tang, Y. N. Xiao, L. Chen, and R. A. Cheke, "Integrated pest management models and their dynamical behaviour," *Bulletin of Mathematical Biology*, vol. 67, no. 1, pp. 115–135, 2005.

[25] S. Y. Tang and J. H. Liang, "Global qualitative analysis of a non-smooth Gause predator-prey model with a refuge," *Nonlinear Analysis, Theory, Methods and Applications*, vol. 76, no. 1, pp. 165–180, 2013.

[26] S. Y. Tang, Y. N. Xiao, and R. A. Cheke, "Dynamical analysis of plant disease models with cultural control strategies and economic thresholds," *Mathematics and Computers in Simulation*, vol. 80, no. 5, pp. 894–921, 2010.

[27] C. Dai and M. Zhao, "Mathematical and dynamic analysis of a prey-predator model in the presence of alternative prey with impulsive state feedback control," *Discrete Dynamics in Nature and Society*, vol. 2012, Article ID 724014, 19 pages, 2012.

[28] J. C. Brumberg and B. S. Gutkin, "Cortical pyramidal cells as non-linear oscillators: experiment and spike-generation theory," *Brain Research*, vol. 1171, no. 1, pp. 122–137, 2007.

[29] J. Guckenheimer and R. A. Oliva, "Chaos in the Hodgkin-HUXley model," *SIAM Journal on Applied Dynamical Systems*, vol. 1, no. 1, pp. 105–114, 2002.

[30] J. Rinzel and R. N. Miller, "Numerical calculation of stable and unstable periodic solutions to the Hodgkin-HUXley equations," *Mathematical Biosciences*, vol. 49, no. 1-2, pp. 27–59, 1980.

[31] R. Llinas and M. Sugimori, "Electrophysiological properties of in vitro Purkinje cell somata in mammalian cerebellar slices," *The Journal of Physiology*, vol. 305, pp. 171–195, 1980.

[32] Y. Mandelblat, Y. Etzion, Y. Grossman, and D. Golomb, "Period doubling of calcium spike firing in a model of a Purkinje cell dendrite," *Journal of Computational Neuroscience*, vol. 11, no. 1, pp. 43–62, 2001.

[33] R. Rakkiyappan, A. Chandrasekar, J. H. Park, and O. M. Kwon, "Exponential synchronization criteria for Markovian jumping neural networks with time-varying delays and sampled-data control," *Nonlinear Analysis: Hybrid Systems*, vol. 14, pp. 16–37, 2014.

[34] S. Coombes, R. Thul, and K. C. Wedgwood, "Nonsmooth dynamics in spiking neuron models," *Physica D. Nonlinear Phenomena*, vol. 241, no. 22, pp. 2042–2057, 2012.

[35] S. Coombes, "Neuronal networks with gap junctions: a study of piecewise linear planar neuron models," *SIAM Journal on Applied Dynamical Systems*, vol. 7, no. 3, pp. 1101–1129, 2008.

[36] H. G. Rotstein, S. Coombes, and A. M. Gheorghe, "Canard-like explosion of limit cycles in two-dimensional piecewise-linear models of FitzHugh-Nagumo type," *SIAM Journal on Applied Dynamical Systems*, vol. 11, no. 1, pp. 135–180, 2012.

[37] A. Tonnelier and W. Gerstner, "Piecewise linear differential equations and integrate-and-fire neurons: insights from two-dimensional membrane models," *Physical Review E*, vol. 67, no. 2, pp. 0219081–02190816, 2003.

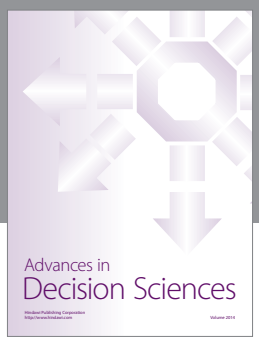

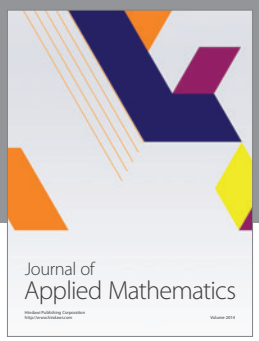

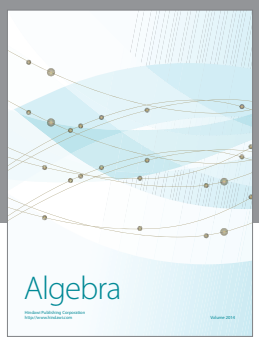

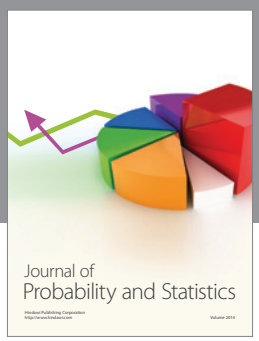

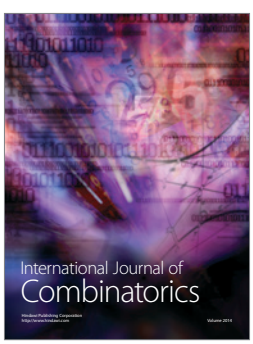

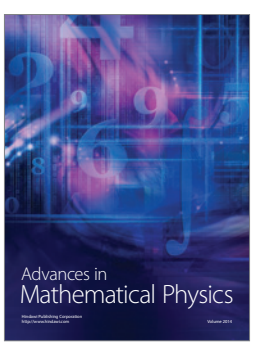

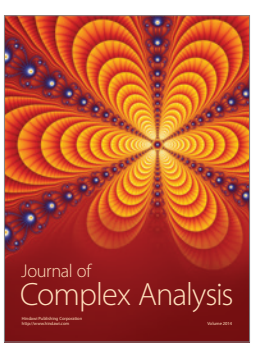

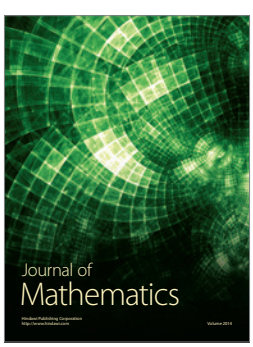

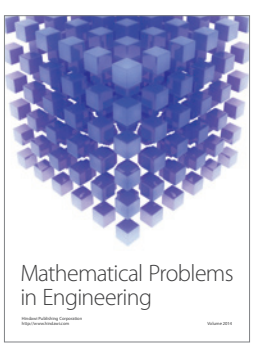

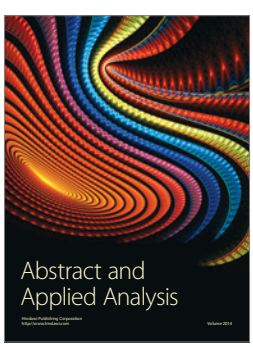

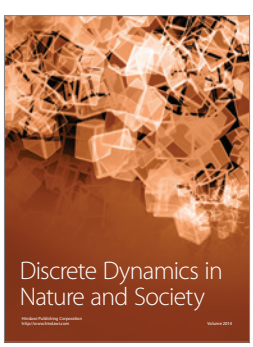

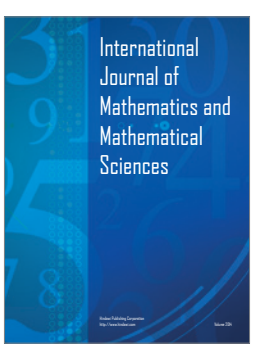

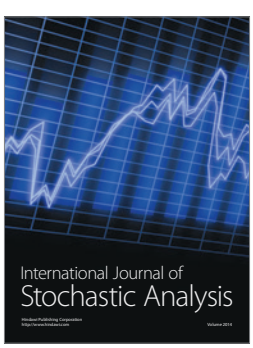

Hindawi

Submit your manuscripts at
http://www.hindawi.com